

Distinct methylation profile of mucinous ovarian carcinoma reveals susceptibility to proteasome inhibitors

Phui-Ly Liew^{1,2}, Rui-Lan Huang^{3,4}, Yu-Chun Weng⁴, Chia-Lang Fang^{2,5}, Tim Hui-Ming Huang⁶ and Hung-Cheng Lai^{3,4,7,8,9}

¹ Department of Pathology, Shuang Ho Hospital, Taipei Medical University, New Taipei, Taiwan

² Department of Pathology, School of Medicine, College of Medicine, Taipei Medical University, Taipei, Taiwan

³ Department of Obstetrics and Gynecology, Shuang Ho Hospital, Taipei Medical University, New Taipei, Taiwan

⁴ Translational epigenetic center, Shuang Ho Hospital, Taipei Medical University, New Taipei, Taiwan

⁵ Department of Pathology, Wan Fang Hospital, Taipei Medical University, Taipei, Taiwan

⁶ Department of Molecular Medicine/Institute of Biotechnology, University of Texas Health Science Center at San Antonio, San Antonio, TX

⁷ Department of Obstetrics and Gynecology, School of Medicine, College of Medicine, Taipei Medical University, Taipei, Taiwan

⁸ Department of Clinical Pharmacology, Xiangya Hospital, Central South University, Changsha 410008, People's Republic of China

⁹ Hunan Key Laboratory of Pharmacogenetics, Institute of Clinical Pharmacology, Central South University, Changsha 410078, People's Republic of China

Mucinous type of epithelial ovarian cancer (MuOC) is a unique subtype with a poor survival outcome in recurrent and advanced stages. The role of type-specific epigenomics and its clinical significance remains uncertain. We analyzed the methylomic profiles of 6 benign mucinous adenomas, 24 MuOCs, 103 serous type of epithelial ovarian cancers (SeOCs) and 337 nonepithelial ovarian cancers. MuOC and SeOC exhibited distinct DNA methylation profiles comprising 101 genes, 81 of which exhibited low methylation in MuOC and were associated with the response to glucocorticoid, ATP hydrolysis-coupled proton transport, proteolysis involved in the cellular protein catabolic process and ion transmembrane transport. Hierarchical clustering analysis showed that the profiles of MuOC were similar to colorectal adenocarcinoma and stomach adenocarcinoma. Genetic interaction network analysis of differentially methylated genes in MuOC showed a dominant network module is the proteasome subunit beta (*PSMB*) family. Combined functional module and methylation analysis identified *PSMB8* as a candidate marker for MuOC. Immunohistochemical staining of *PSMB8* used to validate in 94 samples of ovarian tumors (mucinous adenoma, MuOC or SeOC) and 62 samples of gastrointestinal cancer. *PSMB8* was commonly expressed in MuOC and gastrointestinal cancer samples, predominantly as strong cytoplasmic and occasionally weak nuclei staining, but was not expressed in SeOC samples. Carfilzomib, a second-generation proteasome inhibitor, suppressed MuOC cell growth *in vitro*. This study unveiled a mucinous-type-specific methylation profile and suggests the potential use of a proteasome inhibitor to treat MuOC.

Mucinous ovarian tumors represent a distinct spectrum of ovarian neoplasms.¹ Benign mucinous adenoma, mucinous borderline tumor/atypical proliferative mucinous tumor, intraepithelial (noninvasive) mucinous carcinoma, microinvasive mucinous carcinoma and mucinous type of epithelial ovarian cancer (MuOC) can coexist in close proximity within one neoplasm.

Key words: methylation profiles, functional genetic interactions, mucinous ovarian carcinoma, *PSMB8*, proteasome inhibitors

Abbreviations: BRCA: breast carcinoma; COREAD: colorectal adenocarcinoma; DM: differential methylation; DMG: differentially methylated gene; DFS: disease-free survival; EOC: epithelial ovarian cancer; GICA: gastrointestinal cancer; GBM: glioblastoma multiform; LIHC: hepatocellular carcinoma; MethylCap-seq: methyl-CpG binding domain of the MBD2 protein to capture double-stranded DNA followed by high-throughput next-generation sequencing; MuOC: mucinous type of epithelial ovarian cancer; NIK/NF-kappa B: noncanonical nuclear factor kappa-light-chain-enhancer of activated B cells; NOS: non-otherwise specified; OS: overall survival; *PSMB*: proteasome subunit beta; siRNA: small interference double-strand RNA; SFRP5: secreted frizzled-related protein-5; SeOC: serous type of epithelial ovarian cancer; STAD: stomach adenocarcinoma

Additional Supporting Information may be found in the online version of this article.

P.-L.L. and R.-L.H. contributed equally to this work

Grant sponsor: Shuang Ho Hospital-Taipei Medical University; **Grant numbers:** 104TMU-SHH-07, 106TMU-SHH-04, 106TMU-SHH-14;

Grant sponsor: National Health Research Institutes; **Grant number:** NHRI-EX106-10406BI; **Grant sponsor:** Ministry of Science and Technology of Taiwan (MOST); **Grant number:** 105-2628-B-038-011-MY3

DOI: 10.1002/ijc.31324

This is an open access article under the terms of the Creative Commons Attribution-NonCommercial License, which permits use, distribution and reproduction in any medium, provided the original work is properly cited and is not used for commercial purposes.

History: Received 24 Oct 2017; Accepted 5 Feb 2018; Online 8 Mar 2018

Correspondence to: Hung-Cheng Lai, MD, PhD, No. 291, Jhongjheng Rd, Jhonghe, New Taipei 23561, Taiwan, E-mail: hclai30656@gmail.com or hclai@s.tmu.edu.tw

What's new?

Epigenetic changes such as DNA methylation play an important role in cancer development. In this study, the authors found that mucinous epithelial ovarian cancers (MuOC) display changes in methylation similar to those seen in colorectal and gastric cancers, especially in the proteasome system. They also found that a proteasome subunit called PSMB8 may provide a useful diagnostic marker for MuOC, and that proteasome inhibitors blocked the growth of MuOC cells. These results suggest that the proteasome system may offer a useful target for both diagnosis and treatment of MuOC.

Although the tubal origin of high-grade serous ovarian cancer is known, the cell of origin of mucinous tumors in the ovary is unknown. It has been proposed that mucinous tumors may arise from mature teratomas² and non-germ-cell origin from Brenner tumors near the tuboperitoneal junction.^{3,4}

After systematic review to exclude metastatic lesions from gastrointestinal, pancreatic or other gynecologic primary tumors, the true incidence of primary MuOC is up to 12%.¹ In contrast to the late diagnosis of high-grade serous type of epithelial ovarian cancer (SeOC), 83% of MuOC cases are FIGO stage I at the time of the initial diagnosis. Patients with stage I MuOC have a 5-year survival rate of 91%, whereas patients with recurrent disease or those diagnosed in an advanced stage usually die of the disease. The prognosis is significantly worse for patients with advanced-stage MuOC than for patients with other histological subtypes of advanced-stage ovarian cancer.⁵ The reason for this appears to be related to the frequency of platinum resistance in patients with MuOC.⁶ Although the difference in clinical behavior is obvious, specific treatments for mucinous-type cancers do not currently exist.

Attention is now focusing on the discovery of driver mutations that may be useful in targeted therapy, and certain genetic mutations have been identified in MuOC.⁷ The molecular landscape of MuOC is poorly understood because of the rarity of these tumors and insufficient sample sizes for comprehensive mutation and expression analyses. At least three hypotheses are possible. First, most MuOCs could develop along a low-grade pathway by acquisition of alterations in the mitogen-activated protein kinase (MAPK) cascade (e.g., in *KRAS*). Second, a subset of mucinous tumors with a change in the MAPK pathway could eventually progress to a high-grade mucinous carcinoma through a further change-of-function mutation at *TP53*. Third, a postulated subset of MuOCs could develop as high grade from the start, similar to the development of high-grade serous ovarian carcinogenesis, with a mutation in *TP53* but not within the MAPK pathway.

KRAS mutations are the most common genetic event in 50% of mucinous borderline tumors and in 60% of primary MuOCs.^{8–12} *HER2* amplification is common in patients with MuOC (18.2%).¹³ Mutations of *TP53* have been found in up to 97% of serous cancers, although only 16% of mucinous cancers harbor mutated *TP53*. These genetic events confer no prognostic value for patients undergoing standard therapies.

Nuclear expression of β -catenin, which is indicative of aberrant signaling in the wingless (*WNT*) pathway, was reported in 9% of MuOC cases.

Epigenetic changes play an important role in cancer development.^{14,15} Epigenetic silencing of tumor suppressor genes by promoter hypermethylation is commonly observed in human cancers.^{16,17} DNA methylation may serve as a marker for the differential diagnosis of cancer and as a means of assessing the prognosis of cancer patients.^{18–21} Aberrant DNA methylation is a common epigenetic event leading to the inactivation of tumor suppressor genes in ovarian cancer.^{22,23} In addition, hypermethylation of many genomic regions associated with transcriptional silencing has also been shown in different histological subtypes of ovarian cancer.^{24,25} So far, studies of DNA methylation in ovarian cancer are limited and have not produced useful information for clinical application.^{25–28} The effects of epigenetic modifications are tissue specific. Understanding the epigenome of specific tissue types may lead to the development of novel therapeutics.

In this study, we hypothesized that MuOC shares the same epigenetic methylation sequence as colorectal adenocarcinoma (COREAD) and stomach adenocarcinoma (STAD), and that this methylation pattern differs from that of benign mucinous adenoma and SeOC. We have discovered a proteasome pathway as a newly identified and common unmethylation event for MuOC, COREAD and STAD. Our data suggest that the proteasome subunit beta type-8 (PSMB8) inhibitor has potential as an indicator of MuOC in women.

Materials and Methods**Methylomic datasets and differential methylation analysis**

For identification of the differential methylation (DM) profiles between MuOC and SeOC, we used two methylomic datasets of ovarian tumors. The first dataset was our methyl-CpG binding domain of the MBD2 protein to capture double-stranded DNA followed by high-throughput next-generation sequencing (MethylCap-seq) dataset, which included MuOC ($n = 16$), SeOC ($n = 50$) and benign mucinous adenoma ($n = 6$) (Supporting Information, Table S1). We performed the methylation level by sequencing of fragmentally methylated DNA.²⁹ Another dataset was deposited in NCBI's Gene Expression Omnibus (GEO) with accession number GSE51820 (<https://www.ncbi.nlm.nih.gov/geo/query/acc.cgi?acc=GSE51820>). The GSE51820 dataset included

methylomic data of MuOC ($n = 8$) and SeOC ($n = 53$) generated by HumanMethylation450 BeadChip.³⁰ We used two-sided Student's *t* test to identify DM level between MuOC and SeOC. In MethylCap-sequencing dataset analysis, we set $p \leq 0.05$ and DM level ≥ 0.1 normalized reads number (Supporting Information, Table S2). In GSE51820 dataset analysis, we set the DM criteria including $p \leq 0.005$, DM level $\geq 15\%$, and retained probe with numbers of single nucleotide polymorphisms (SNPs) ≤ 1 .

We utilized DAVID (version 6.8, <https://david.ncifcrf.gov/tools.jsp>) as a bioinformatics resource and functional annotation of differentially methylated gene-by-gene ontology (GO) biological process^{31,32} to perform functional enrichment analysis.

Hierarchical clustering analysis of the methylation profiles of malignant tumors from different organs

We analyzed the consensus clustering methylation profiles of seven malignant tumors from six different organs. Totally 398 methylomics data including eight MuOC, 53 SeOC, 105 COREAD, 43 STAD, 68 breast carcinoma (BRCA), 62 glioblastoma multiform (GBM) and 59 hepatocellular carcinoma (LIHC) from Broad Institute GDAC constitutes (<http://gdac.broadinstitute.org/>) were download in 2016. The abbreviations of different carcinoma have followed the record from The Cancer Genome Atlas (TCGA) data portal (<https://tcga-data.nci.nih.gov/docs/publications/tcga/>). The 43 STAD included 20 mucinous type adenocarcinomas and stage/age matched 23 non-otherwise-specified (NOS) adenocarcinomas. The 105 COREAD consisted of 58 conventional adenocarcinomas and 47 mucinous carcinomas. The 68 BRCA enrolled 15 mucinous carcinomas and 53 invasive ductal carcinomas. The patient's barcode and diagnosis were listed in Supporting Information, Table S3. We used the level 3 methylomics data and the results were generated by the TCGA Research Network in whole based upon data. The similarity of methylation profiles was analyzed by unsupervised hierarchical clustering with complete linkage method to calculate the Euclidean distance matrix and build the dendrogram by MeV version 4.9.0.

Functional genetic interactions network of MuOC pathogenesis

To develop the genetic interactions network of DM genes in MuOC, we integrated the BioGRID database and mRNA coexpressed profiles. The BioGRID is a freely accessible database of physical and genetic interactions available at <http://www.thebiogrid.org>.³³ BioGRID has released version 3.4, which includes 21,729 genes and 419,253 known interactions from *Homo sapiens*. We used DM genes to retrieve the first and second level of interactors by the BioGRID database and showed as the node. The first and second level of interactor directly interacts with DM genes and the first level of interactor, respectively. We kept the interactions as the edge of paired nodes by computing the Pearson correlation coefficient from the MuOC transcriptomic data (GSE6008).³⁴ The

interactions were significantly coexpressed with positive correlation coefficient $r \geq 0.55$ and p values < 0.05 . The network visualization was performed by using the software Cytoscape 3.3.0, which was available at <http://www.cytoscape.org/>. The functional network was annotated by DAVID with biology processing term.

Study participants, tissue sections, tissue microarray and immunohistochemistry

From the years 1999 to 2013, totally 94 patients including 27 mucinous ovarian adenomas, 38 MuOCs and 29 SeOCs were retrieved from the archival pathology files of the Taipei Medical University³⁵ and Taipei Medical University Joint Biobank. The hematoxylin and eosin-stained slides were reviewed by two pathologists, and representative blocks with whole tissue sections of ovarian tumors were selected for immunohistochemistry (Supporting Information, Table S4). The primary ovarian tumors were classified according to the current World Health Organization criteria.¹ The surgical procedures included total hysterectomy, bilateral salpingo-oophorectomy, pelvic and/or para-aortic lymph nodes sampling and omentectomy. Tissue microarrays were constructed from 62 gastrointestinal cancer patients (30 STADs and 32 COREADs) at Taipei Medical University (Supporting Information, Table S5). We retrieved two to three representative 2.5–3.0 mm tumor cores of formalin-fixed paraffin-embedded tissue (tumor area identified by pathologist). Demographic, intraoperative and clinical follow-up data were obtained from hospital electronic charts under the guidelines of the Taipei Medical University Institutional Review Board (Protocol #N201607012).

Tissue slides were stained with monoclonal antihuman proteasome subunit beta type 8 antibody (PSMB8, WH000566M1, dilution 1:200, Sigma). Clinicopathological features were analyzed for differences in PSMB8 expression. The tissue samples used for MethylCap-seq and immunohistochemistry were different groups of patients and these samples were analyzed independently. The percentages of positive cells (nucleus and/or cytoplasm) were recorded. The intensity of positive staining cells (nucleus and/or cytoplasm) were scored as negative (score 0), weak (score 1) and strong (score 2). The total scores of positively stained cells were assessed, and a formula calculated as follows: (percentage) \times (intensity score). Cases with 100 or > 100 scores of tumor cells staining with PSMB8 were considered high expression, and cases with < 100 scores of tumor cells were considered low expression. There were 2 distinctive expression patterns for PSMB8: cytoplasmic staining and nucleus staining. We evaluated the expression pattern for cytoplasmic expression in the cases of MuOC, COREAD and STAD, respectively.

Disease status was defined as follows: (i) dead of disease: patient died as a result of persistent, progressive or recurrent disease; (ii) alive with disease: patient alive with clinical and/or radiographic evidence of persistent, progressive or recurrent disease; (iii) dead of intercurrent disease: patient died

from an unrelated cause with no clinical or radiographic evidence of persistent, progressive or recurrent disease; (iv) no evidence of disease. Disease-free survival (DFS) was measured in months from the date of initial diagnosis to the date of first evidence of tumor recurrence or progression. Overall survival (OS) was measured in months from the date of initial diagnosis to the date of death or date of last follow-up.

Cell lines and culture conditions

Totally seven human epithelial ovarian cancer (EOC) cell lines, including MCAS, EFO-27, EFO-27 and its subclone (EFO-27*), Kuramochi and PEO1 were obtained from Ruby Yun-Ju Huang³⁶; OVCAR3 and SKOV3 were purchased previously.³⁷ The serous type of EOC cell lines were SKOV3, OVCAR3, Kuramochi and PEO1, which were cultured in RPMI-1640 (Invitrogen) with 10% standard fetal bovine serum (FBS, Biological Industries). The MCAS, EFO-27 and EFO-27* were mucinous type of EOC cell lines, which were maintained in culture medium in RPMI-1640 with 20% FBS and DMEM (Invitrogen) with 15% FBS, respectively. Cells were confirmed the DNA profiling of short tandem repeat (STR) sequences were by the MISSION BIOTECH (Taipei, Taiwan). DNA profiles were compared manually the STR information released at the websites of ATCC, JCRB and European Collection of Authenticated Cell Cultures (ECACC).

Protein and mRNA expression analysis

For evaluating the mRNA expression of *PSMB8*, the real-time PCR was used to measure reversed cDNA from mRNA and recognized by paired primers, which were 5'-GCAGG-CTGTACTATCTGCGAA-3' and 5'-AGAGCCGAGTCCCA-TGTTTCAT-3'. The mRNA was extracted from cells using RNeasy Mini Kit (QIAGEN), and reversed to cDNA using Transcriptor First Strand cDNA Synthesis Kit (Roche) with random hexamer primer. The PCR products were amplified with the LightCycler 480 SYBR Green I Master (Roche) and performed using LightCycler 480. A 20 μ l reaction contained 20 ng cDNA, 250 nM of each primer and 10 μ l Master Mix. PCR conditions were denaturation at 95°C for 5 min, 45 polymerization cycles, which following 95°C for 10 s, 60°C for 30 s and 72°C for 30 s, and final extension at 72°C for 5 min and collect data under duplicate procedure. The $\Delta\Delta CT$ was calculated using the housekeeping gene *GAPDH* as a reference.

For evaluating the protein expression of *PSMB8*, western blots used to explore the candidate proteins with total cell lysates according to a standard protocol by using polyclonal anti-*PSMB8* antibody (HPA046995, dilution 1:200, ATLAS). Proteins were visualized using commercially available secondary antibody anti-rabbit-IgG or anti-mouse-IgG (GeneTex) and ECL chemiluminescent (Thermo Scientific Pierce) for development. Rabbit anti- β -actin antibody was purchased from GeneTex and used as loading control.

Transfection, cell viability and chemosensitivity assay

Small interference double-strand RNA (siRNA pool, M-006022-01-0005) against the *PSMB8* gene and nontarget siRNA as control were purchased from Dharmacon. The cell viability assay was performed by seeding 1,000 cells in 96-well plates with complete media and detected at 0, 24, 48, 72 and 128 hr. After adding 3-(4,5-dimethylthiazol-2-yl)-2-(4-sulfophenyl)-2 H-tetrazolium reagents (Promega) for 1 hr, each well was measured the absorbance using OD 490 nm in MultiSKAN Ex ELISA reader (Thermo Scientific Pierce). The chemosensitivity assay was performed by seeding 1,000 cells in 96-well plates with complete media and detected in adding 0, 1, 2, 4, 8, 16, 32, 64, 128 and 256 nM Carfilzomib or Bortezomib (Apexbio). The Carfilzomib or Bortezomib are proteasome inhibitors. Carfilzomib targets *PSMB* 1, 2, 5, 8, 9 and 10. Bortezomib specifically inhibits *PSMB*1 and *PSMB*5.

Statistical analysis

Correlations between categorical clinical variables and methylation level were identified by Fisher's exact test for 2×2 categories and the Freeman-Halton extension of Fisher's exact probability test for 3×2 categories. All significant differences were assessed using a two-sided $p \leq 0.05$. Above analyses and plots were performed using the statistical package in R (version 3.3.2) and MedCalc (version 17.0.14).

Results

Differences in DNA methylation profiles between MuOC and SeOC

To identify unique DNA methylation profiles of MuOC, we compared two methylomic profiles between MuOC and SeOC. One was the MethylCap-seq dataset, which included 16 MuOC and 50 SeOC samples; and the other was the BeadChip dataset, which included eight MuOC and 53 SeOC samples. In the MethylCap-seq dataset, 2231 low differentially methylated genes (DMGs) and 410 high DMGs were identified as significant in MuOC samples. In the BeadChip dataset (GSE51820), 293 low DMGs and 193 high DMGs were significant. We intersected the selected DMGs to find 81 commonly low DMGs and 20 high DMGs (Fig. 1a and Supporting Information, Table S2).

Hierarchical clustering analysis was used to identify similarities between MuOC and SeOC based on the methylation profiles of 101 DMGs in the two datasets (Figs. 1b and 1c). In the MethylCap-seq dataset, the dendrogram showed clusters containing two groups. One cluster grouped all cases of MuOC and some SeOC, whereas another cluster grouped only the SeOC cases (Fig. 1b). In the BeadChip dataset, the dendrogram also identified two clusters. One cluster grouped only MuOC cases, and the other cluster grouped all SeOC cases and an MuOC (Fig. 1c). The methylation profiles of the 101 DMGs successfully discriminated MuOC from SeOC. Functional enrichment analysis of the 101 DMGs according to their biological processes revealed response to glucocorticoid,

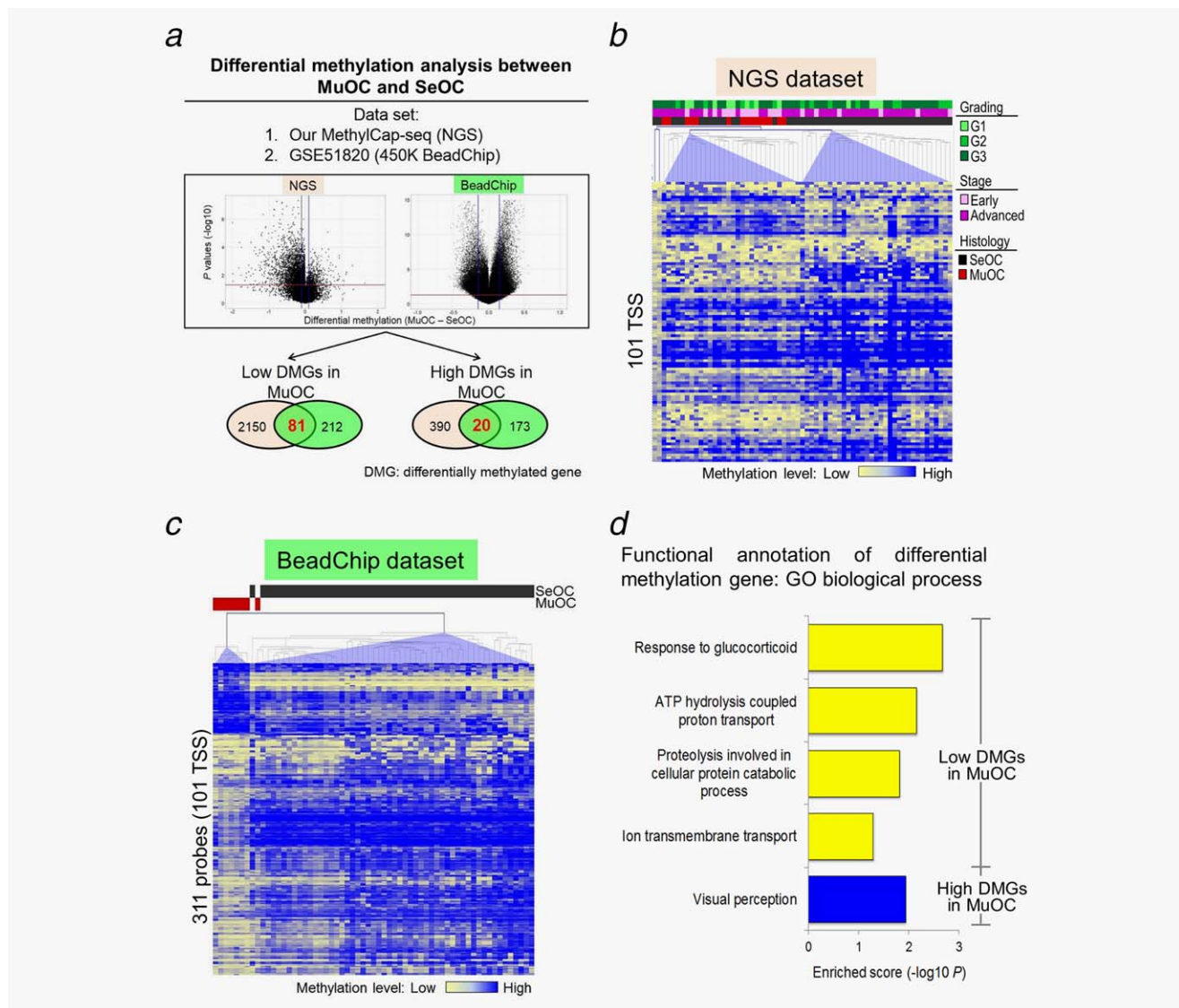


Figure 1. Identification of different DNA methylation profiles between mucinous type of epithelial and serous type of epithelial ovarian cancer. (a) Distribution of differential DNA methylation profiles between MuOC and SeOC in two datasets. One dataset included the methyl-CpG-binding domain of the MBD2 protein to capture double-stranded DNA followed by high-throughput next-generation sequencing (MethylCap-seq) (NGS). The other dataset was GSE51820, which was obtained using the Methylation 450k BeadChip. We identified 81 low differentially methylated genes (DMGs) and 20 highly DMGs in MuOC. (b) The MethylCap-Seq (NGS) dataset showed two clusters of DNA methylation at the transcription start site (TSS) of 101 DMGs. One cluster selected all cases of MuOC and some SeOC cases, and the other selected only SeOC cases. (c) Two separate DNA methylation clusters of MuOC and SeOC were detected in the BeadChip dataset. (d) Functional annotation of DMGs in MuOC by biological process of gene ontology (GO). The top four significance of enriched functions in low DMGs were related to the response to glucocorticoid, ATP hydrolysis-coupled proton transport, proteolysis involved in cellular protein catabolic process and ion transmembrane transport. The biological process of visual perception is only enriched in high DMGs.

ATP hydrolysis-coupled proton transport, proteolysis involved in cellular protein catabolic process, and ion transmembrane transport in the low DMGs and visual perception in the high DMGs (Fig. 1d and Supporting Information, Table S6). Taken together, these differences in the methylomic profiles between MuOC and SeOC suggest that they represent different biological processes, which may lead to heterogeneity of ovarian cancers.

Similarity between MuOC and gastrointestinal cancer. To test the hypothesis that MuOC is similar to gastrointestinal

cancer (GICA) from a molecular perspective, we used hierarchical clustering analysis to analyze the methylation profiles of 101 DMGs (including 274 CpG sites) in 398 cancer samples. These cancer samples included 8 MuOC, 53 SeOC, 105 COREAD, 43 STAD and 189 non-GICA cases (Fig. 2). The left panel of Figure 2 illustrated the location of the primary carcinomas used in this study. The middle panel showed the tags to identify various types of carcinoma. The right panel showed the dendrogram and methylation level for each sample. The dendrogram showed six clusters.

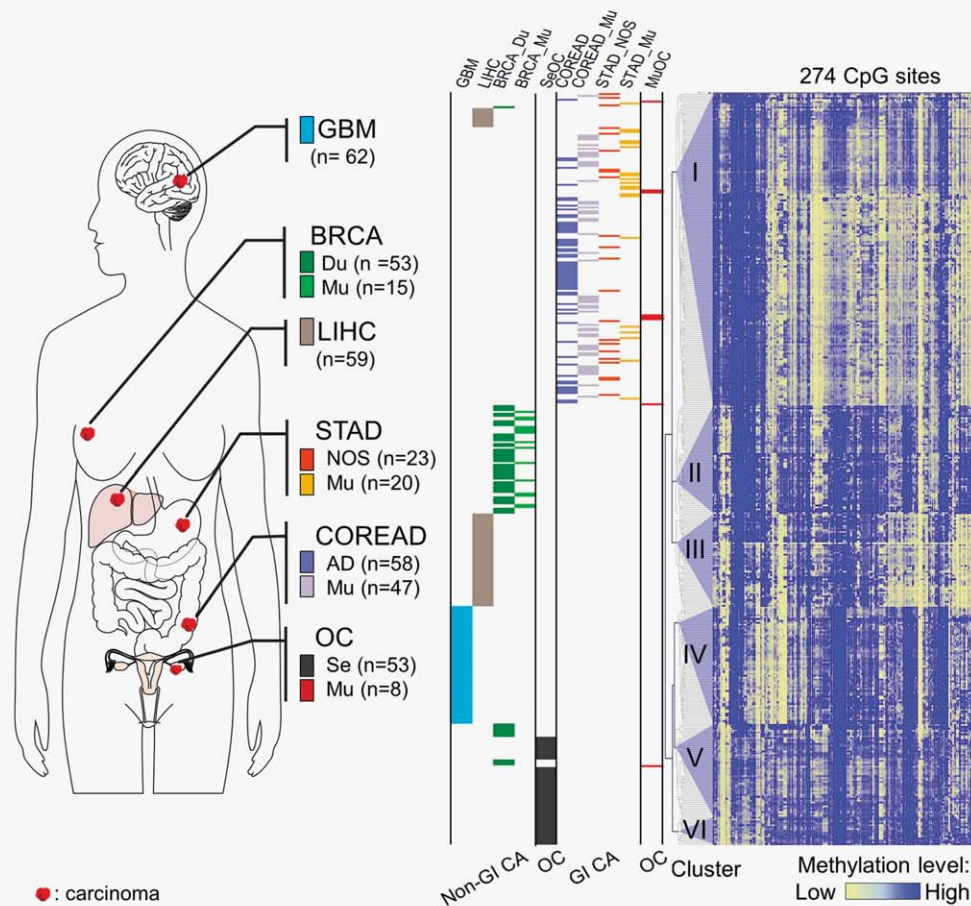


Figure 2. Hierarchical clustering analysis of the methylation profiles on the distinction of different carcinoma. The DNA methylation profiles of 274 CpG sites of 101 genes in 398 cancer samples: 8 MuOCs, 53 serous type epithelial ovarian cancers (SeOCs), 105 COREAD, 43 STAD and 189 nongastrointestinal cancers (non-GI CA). Six clusters of methylation patterns were identified. The left panel illustrated the location of the primary carcinomas used in this study. The middle panel showed the tags for identification of various types of carcinoma. The right panel demonstrated the dendrogram of the similarity by methylation profiles. The first and largest cluster included COREAD, STAD, and almost all MuOC cases. The mucinous subtypes of COREAD and STAD were also grouped together in the same cluster. The second, third, and fourth clusters included breast carcinoma (BRCA) (including ductal and mucinous phenotypes), hepatocellular carcinoma (LIHC) and glioblastoma multiforme (GBM), respectively. The fifth cluster grouped SeOC, a few cases of BRCA, and one MuOC. The sixth cluster grouped partial SeOC cases. *n* is the case number.

Cluster I grouped all cases of COREAD, STAD and all MuOC cases except one. Clusters II, III and IV grouped breast carcinoma (BRCA), hepatocellular carcinoma (LIHC) and glioblastoma multiforme (GBM), respectively. SeOC was grouped into clusters V and VI. These results suggest that MuOC shares some common methylation profiles with COREAD and STAD, but not others, which suggests a common origin or common pathways in cancer development.

Functional network in MuOC pathogenesis

To determine how DMGs contribute to MuOC pathogenesis, we next used the physical and genetic interactions from the BioGRID database,³³ and integrated the coexpression of mRNA profiles,³⁴ to identify the functional network of DMGs and their interactors. The entire functional and three

separately predominant functional networks are shown in Figure 3a. The first subnetwork was involved in thyroid hormone signaling, which included a low-DMG, nuclear receptor coactivator 2 (*NCoA-2*), and two interactors: thyroid hormone receptor beta (*THRβ*) and *NOTCH3* (Fig. 3b). The second subnetwork involved two low-DMGs, *PSMB8* and kazrin, periplakin interacting protein (*KAZN*), which interacts with ELAV-like binding protein 1 (*ELAVL1*) and eukaryotic translation initiation factor 4 gamma 1 (*EIF4G1*) (Fig. 3c). Importantly, the main of functional module includes members of the PSMB family (*PSMB8*, *PSMB9*, *PSMB10* and *PSMB2*). This proteasome module in the aquamarine node border serves as a mediator between both the noncanonical nuclear factor kappa-light-chain-enhancer of activated B cells (*NIK/NF-κB*) pathway and antigen presentation of exogenous antigen via MHC class I (through interaction with the

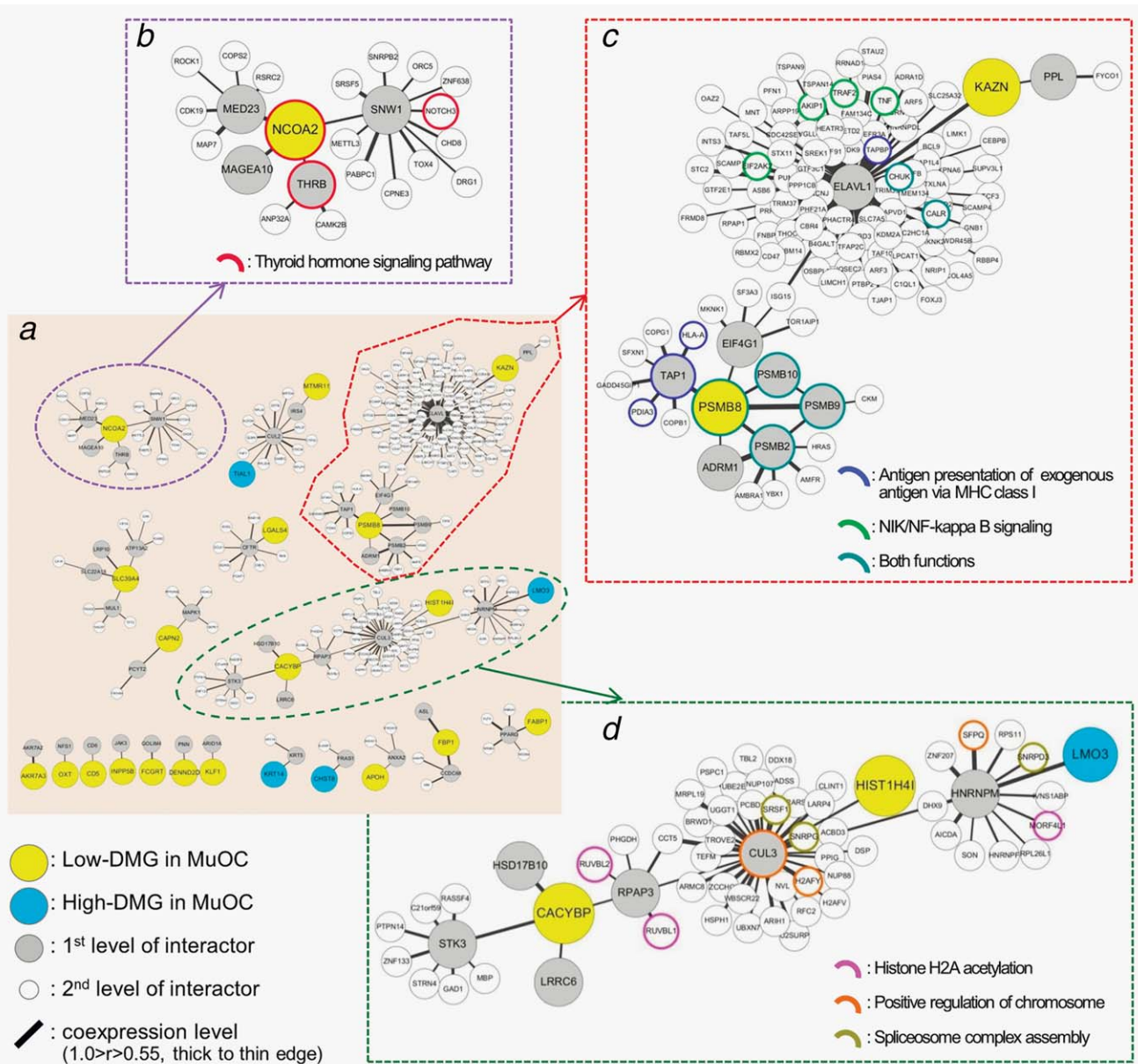


Figure 3. Functional networks of differentially methylated genes in mucinous type epithelial ovarian cancer (MuOC). (a) Genetic interactions network of MuOC pathogenesis. The functional network constructed by the gene coexpression between the differential methylated genes (DMGs) and interactors. (b) The first subnetwork included a low DMGs (nuclear receptor coactivator 2, *NCoA-2*) and its' interactors, which related to the thyroid hormone signaling pathway. (c) The second and largest subnetwork comprised the predominant proteasome subunit beta (PSMB)-type family module, including *PSMB 8*, *PSMB 2*, *PSMB 9* and *PSMB 10*. The proteasome module and interactors were related to both antigen presentation of exogenous antigen via major histocompatibility complex (MHC) class I and to the noncanonical nuclear factor kappa-light-chain-enhancer of activated B cells (NIK/NF-κB) signaling pathway. (d) The third subnetwork included three DMGs (*CACYBP*, *HIST1H4I* and *LMO3*) and their interactors were related to histone H2A acetylation, positive regulation of chromosome and spliceosome complex assembly. The *r* value was calculated as a Pearson correlation coefficient of the transcriptomics data (GSE6008) with $p < 0.05$.

transporter associated with antigen processing 1 [*TAP1*]). The third subnetwork involved in the regulator of the mRNA transcriptional process, which includes low-DMGs (calcyclin-binding protein, *CACYBP* and histone H4, *HIST1H4I*), and a high-DMG (LIM domain only 3, *LMO3*) (Fig. 3d). Our findings epigenetic effects of functional pathways may be leading

to heterogenesis of EOCs and suggest that MuOC may have a lineage that is distinct from that of other EOCs.

PSMB8 may be a specific marker for MuOC

To narrow the candidate targets for therapeutic intervention, we used the MethylCap-seq dataset to compare the DMGs

between malignant and benign mucinous neoplasms and tried to identify the genes that are significantly involved in malignant phenotypes. We found 109 low DMGs and 1253 high DMGs in the MuOC samples in the database (Supporting Information, Fig. S1). We then intersected the DMGs results for MuOC, SeOC and benign mucinous adenoma. Interestingly, we found only two genes in the intersection of the low DMGs: secreted frizzled-related protein-5 (*SFRP5*) and *PSMB8*. We found no intersection for high DMGs. To study further the therapeutic purpose, we subjected *PSMB8* to further validation.

PSMB8 protein expression in ovarian tumor and gastrointestinal cancer

PSMB8 immunohistochemical staining was analyzed in whole-tissue sections from 94 women diagnosed with ovarian tumors, which included 27 benign mucinous adenomas, 38 MuOCs and 29 high-grade SeOCs (Supporting Information, Table S4). The tissue microarrays in 62 cases of GICAs included 32 COREAD and 30 STAD cases (Supporting Information, Table S5). None of the samples of SeOC expressed immunoreactivity for *PSMB8* (Fig. 4) and summarized in Supporting Information, Tables S7 and S8. *PSMB8* cytoplasmic and/or nuclear staining was observed in the MuOC, COREAD and STAD samples (Fig. 4a). Only one of 27 samples of benign mucinous adenoma showed a focal weak cytoplasmic staining pattern (Figs. 4b and 4c). Kaplan–Meier analysis of the data for MuOC samples showed no significant adverse effect on OS or DFS when stratified according to *PSMB8* expression (data not shown) (Table 1). In addition, MuOC samples demonstrated broader cytoplasmic ($p < 0.001$) and nuclear ($p = 0.028$) expression of *PSMB8* and stronger cytoplasmic ($p < 0.001$) and nuclear ($p = 0.016$) expression of *PSMB8* than did COREAD samples (Supporting Information, Tables S7 and S8). Broader cytoplasmic ($p = 0.001$) and stronger cytoplasmic ($p < 0.001$) *PSMB8* staining were also observed in MuOC compared with STAD samples (Figs. 4b and 4c; Supporting Information, Tables S7 and S8). The greater cytoplasmic and nuclear *PSMB8* expression seemed to be associated with a higher nuclear grade of COREAD ($p = 0.022$, Supporting Information, Table S9). No significant differences in *PSMB8* expression were associated with nuclear grade, stage or early recurrence rate in STAD samples (Supporting Information, Table S10). Taken together, the protein level of *PSMB8* is similar to the groupings of methylation profiles. *PSMB8* expressed in MuOC, COREAD and STAD did not express in SeOC and benign mucinous adenomas.

Growth restriction in *PSMB8*-knockdown mucinous-type EOC cells

To examine the functional relevance of *PSMB8* in MuOC, *PSMB8* expression in various EOC cell lines was determined by western blot and mRNA analyses. Among the seven EOC cell lines examined, the expression of *PSMB8*

was higher in three MuOC cell lines, MCAS, EFO-27 and EFO-27*, than in other types of EOC cells (Figs. 5a and 5b). We next performed functional analysis of *PSMB8* in MCAS, EFO-27 and EFO-27* cells, and found that *PSMB8* expression was successfully knocked down by siRNA ($p < 0.05$) (Fig. 5c). As shown in Figure 5d, *PSMB8* knockdown significantly inhibited MCAS, EFO-27 and EFO-27* cell proliferation ($p < 0.01$). MCAS, EFO-27 and EFO-27* cells were exposed to a proteasome inhibitor (Bortezomib or Carfilzomib), all of which inhibited cell proliferation (Fig. 5e).

Discussion

The study of rare ovarian tumors is challenging, but understanding the histological and molecular similarities between different cancers, regardless of organ site, may help identify new treatment targets. Mucinous ovarian tumors represent an unusual tumor type that shows an apparent transition from benign to borderline to invasive carcinoma. The diagnosis and treatment of advanced stage or recurrent MuOC are two major challenges. The prognosis of early stage MuOC is good, but the greatest opportunity for cure depends on the use of state-of-the-art surgery. The outcome is much worse for patients with advanced disease or recurrent MuOC. The evidence base for postsurgical adjuvant chemotherapy for advanced or recurrent MuOC is lacking. In addition, mucinous tumors are less sensitive to treatment with commonly used platinum-based chemotherapy. Research to identify new and better therapeutic agents for ovarian mucinous tumors is vital.

The molecular pathways leading to the development of MuOC are not well understood. This study examined two sets of DNA methylation profiles to identify DM patterns in MuOC and SeOC. We confirmed that MuOC is a distinct ovarian cancer because it harbors a different methylation profile from the most common EOC subtype SeOC. In our study, the methylation profiles of 101 genes successfully discriminated MuOC from SeOC. Functional enrichment analysis showed the low DMGs of MuOC were associated with the response to glucocorticoid, ATP hydrolysis-coupled proton transport, proteolysis involved in the cellular protein catabolic process and ion transmembrane transport. These findings indicate the need for MuOC-specific molecular therapeutic drugs that are different from those used to treat SeOC because these two types of cancer have diversely epigenetic effects during cell development.

We next analyzed the consensus clustering methylation profiles of seven malignant tumors from six different organs. We have shown for the first time that MuOC, COREAD (including conventional and mucinous subtypes) and STAD (including NOS and mucinous subtypes) shared similar epigenetic methylation profiles as compared with four other malignant tumors. Mucinous carcinomas of the ovary and colorectum exhibit similarities that include frequent *KRAS* mutations, *HER2* amplification, unfavorable outcome in the advanced stage and minimal response to conventional (GICA or EOC-based) chemotherapy.^{38,39} Our findings suggest

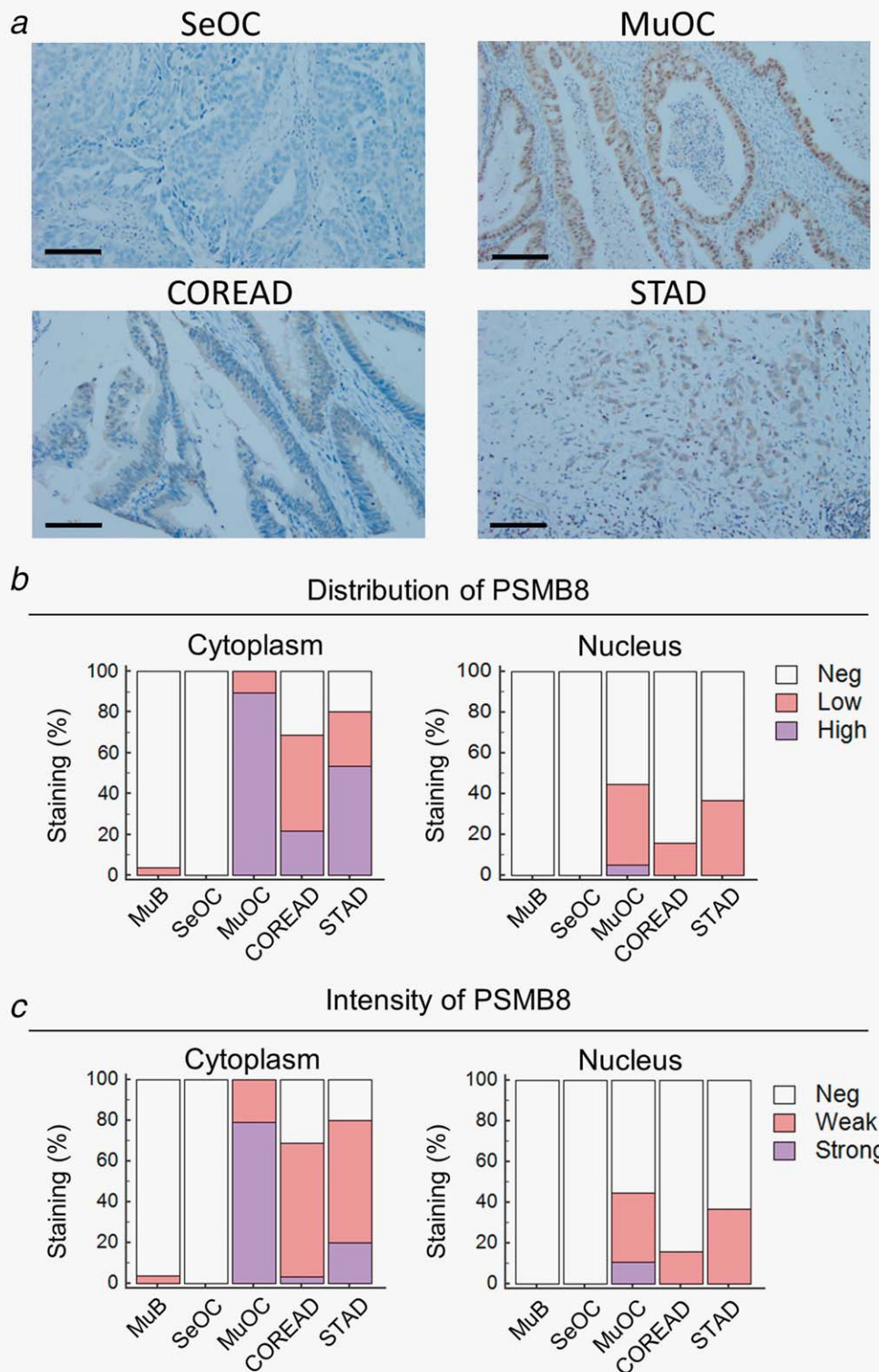


Figure 4. Immunohistochemistry of PSMB8. (a) Serous type epithelial ovarian cancer (SeOC) was negative (Neg). PSMB8 staining was localized to both the cytoplasm and nuclei in mucinous type epithelial ovarian cancer (MuOC), colorectal adenocarcinoma (COREAD) and stomach adenocarcinoma (STAD). (b and c) PSMB8 staining frequency and intensity distributions in all tissue samples. Scale bar = 200 μ m.

further that MuOC, COREAD and STAD might originate from the same cell type,^{40,41} irrespective of the mucinous phenotype of each anatomical site.

We also compared the profiles of DMG in mucinous carcinoma from different organs. However the profile of mucinous carcinoma of the breast was differed from that of MuOC,

Table 1. Clinicopathologic features stratified by proteasome subunit beta type 8 (PSMB8) expression in mucinous type of epithelial ovarian cancer (MuOC)

Clinical and pathologic features		PSMB8 expression		
		Low	High	<i>p</i> value
Age (mean ± SD)		41.3 ± 13.9	51.0 ± 14.8	1.000
	≤60	9	22	
	>60	2	5	
Nuclear grade	Grade 1	6	6	0.219 ¹
	Grade 2	6	17	
	Grade 3	0	3	
FIGO stage	I–II	11	23	1.000
	III–IV	1	3	
Recurrence	No	8	21	1.000
	Yes	3	6	
Recurrent interval	≤12 months	3	2	0.167
	>12 months	0	4	

p values were calculated by Fisher's exact test.

¹Using Freeman–Halton extension method.

COREAD and STAD. These results suggest that mucinous histological characteristics of cancers at different organ sites might not share a common origin or similar molecular alteration. Perhaps most importantly, we have characterized the epigenetic features of MuOC and found that these resembled those of COREAD and STAD, which might be useful for guiding adjuvant treatment options for this rare tumor and for increasing patient survival.

Importantly, our study discovered a dominant of functional module that comprises members of the PSMB family (*PSMB8*, *PSMB9*, *PSMB10* and *PSMB2*) and appears to contribute to MuOC pathogenesis. This module serves as a mediator between the NIK/NF-κB pathway and antigen presentation of exogenous antigen via MHC class I. NIK/NF-κB signaling is aberrantly activated or repressed in many malignancies, autoimmune disorders and bone disorders.⁴² However, roles for the activation of the noncanonical pathway in ovarian cancer cells have not been studied extensively. Previous studies reported that the canonical and noncanonical NF-κB pathways are differentially activated in ovarian cancer cells. Obviously, more work is needed to clarify whether NIK inhibition represents an effective target for ovarian cancer treatment.

In our analysis, the antigen presentation of exogenous antigen via MHC class I interacted with *TAP1*. *TAP1* encodes a subunit of an interferon-γ-inducible heterodimer that binds to peptides cleaved by the proteasome and transports them to be loaded into nascent MHC class I molecules for presentation to cytotoxic T lymphocytes. Defects in the antigen-processing machinery may provide tumor cells with a mechanism to escape immune recognition. Additionally, a previous study suggested that tumor hypomethylation at 6p21.3 with

cis upregulation of genes (including *PSMB8*) enriched in immune response processes, increased CD8 T-cell tumor infiltration and transregulation of genes in immune-related pathways associated with longer time to recurrence of high-grade SeOC.⁴³ The effects on T-cell infiltration in the tumor microenvironment in relation to patient survival and immunotherapeutic strategies in MuOC have not been thoroughly studied.

Among the 81 low DMGs, two candidate genes (*SFRP5* and *PSMB8*) may have a potential role in the carcinogenesis of MuOC as shown for SeOC and benign mucinous adenoma. Our previous study demonstrated that epigenetic silencing of *SFRP5* is related to ovarian cancer progression and chemoresistance.⁴⁴ In this study, we focused on the roles of PSMB8 expression in tissue samples and EOC cell lines. The proteasome system is an important nonlysosomal proteolytic pathway that regulates the cell cycle, proliferation, differentiation and inflammation through the selective degradation of ubiquitinated proteins. A previous study has identified *PSMB8* as an essential component and regulator of inflammation and adipocyte differentiation, and indicated that immunoproteasomes have pleiotropic functions in maintaining the homeostasis of a variety of cell types.⁴⁵ PSMB8 expression was first reported as a predictive prognostic factor in gastric cancer.⁴⁶

We performed immunohistochemical staining of the samples of benign mucinous adenoma, MuOC, SeOC, COREAD and STAD. All cases of SeOC showed negative PSMB8 expression. Our results demonstrate that high PSMB8 expression seems to be related to a high nuclear grade of MuOC. However, among the cases of MuOC and STAD, no significant correlation was found between PSMB8 immunohistochemical expression and nuclear grade, stage, recurrence rate, recurrence interval or survival. In COREAD samples, low cytoplasmic PSMB8 expression correlated significantly with low nuclear grade ($p = 0.022$). Larger studies with more patients are warranted to confirm the prognostic implications of PSMB8 expression in MuOC, COREAD and STAD.

The clinical advantages provided by proteasome inhibitors include improved survival in patients with multiple myeloma since 2003. Bortezomib and Carfilzomib are two U.S. Food and Drug Administration-approved 26S proteasome inhibitors for use in humans. Bortezomib is also the first NF-κB inhibitor to be approved for clinical trials of ovarian cancer treatment. Carfilzomib, which has a greater affinity for proteasomes and lower off-target toxicity, was licensed for treating patients with relapsed and/or refractory multiple myeloma in 2012. However, the efficacy of proteasome inhibitors in treating solid tumors, especially EOCs, has not been elucidated.^{47–49} Our findings offer clues to potential MuOC therapeutic targets by showing that PSMB8 inhibitors suppressed the growth of ovarian mucinous-type cell lines *in vitro*. Carfilzomib targets PSMB1, 2, 5, 8, 9 and 10, whereas Bortezomib specifically inhibits PSMB1 and PSMB5. The EFO-27 and its subclone cell lines were established from a

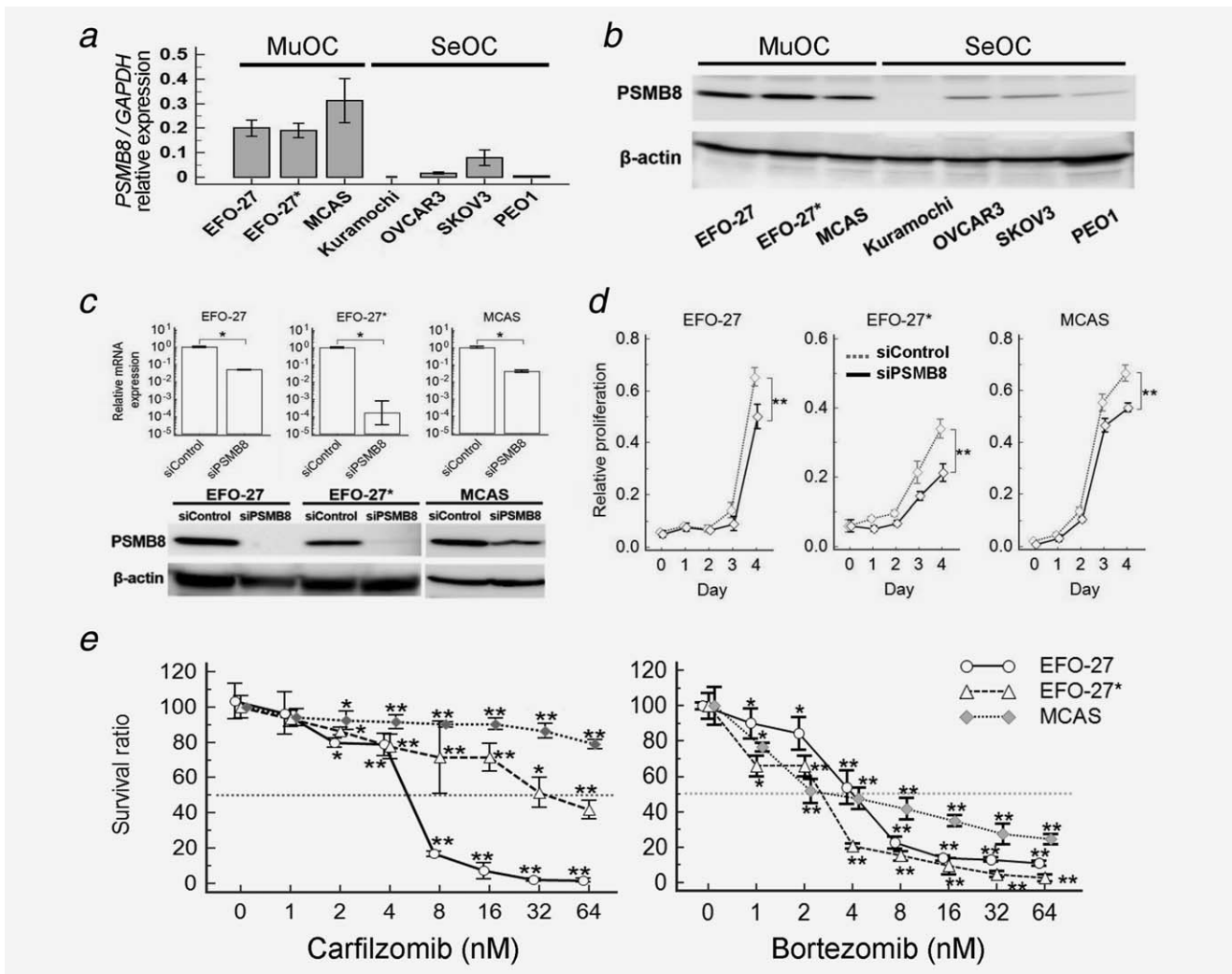


Figure 5. Expression of PSMB8 in different epithelial ovarian cancer (EOC) cells and cytotoxic effect of PSMB8 inhibition in mucinous-type EOC cells. (a and b) Cell lysates from the indicated ovarian cells were subjected to immunoblot analysis with an antibody against PSMB8 and mRNA expression was analyzed. β -Actin was used as a loading control. (c) Small interference (si) double-strand *PSMB8*-transfected and si-Control-transfected MCAS, EFO-27 and its subclone (EFO-27*) cells were evaluated. RT-qPCR and western blot analysis confirmed the low expression of PSMB8 in the cells transfected with *PSMB8* siRNA. (d) *PSMB8* knockdown significantly reduced MCAS, EFO-27 and its subclone (EFO-27*) cell proliferation. (e) Cytotoxic effect of PSMB8 inhibitors (carfilzomib and bortezomib) in mucinous EOC cell lines (five independent experiments were performed and the data were expressed as the means \pm standard deviation, * $p < 0.05$ and ** $p < 0.01$).

solid omental metastasis of a mucinous papillary adenocarcinoma of the ovary with a phosphatase and tensin homolog (*PTEN*) deletion. Although findings from this study warrant replication, they provide intriguing preliminary information on potential therapeutic targets in MuOCs. Future studies designed to assess the predictive value of PSMB8 and response to specific anti-PSMB8 agents in MuOCs are needed.

The proteasome subunit is essential for the regulation of transcription factors through the nuclear localization and promoter interaction mechanisms. A recent study identified the proteasome machinery as a common target of *TP53* missense mutants, which globally affect protein homeostasis and inhibit multiple tumor-suppressive pathways.⁵⁰ Our

study provides a methylomics approach and functional networks for understanding the pathogenesis of and identifying new treatments for MuOC. Further exploration is needed to clarify the molecular mechanisms and to design novel anti-cancer chemotherapies based on the proteasome inhibition of these tumors.

The major limitation of this study is the small tumor tissue sample size of this rare mucinous carcinoma of the ovary. We strictly excluded mucinous borderline tumors because the intratumoral heterogeneity in mucinous ovarian tumors and morphological diagnostic dilemma represent a challenge for epigenetic analyses. Our survival analyses did not show significant correlation with the distribution and intensity of PSMB8 expression. Despite these limitations, we have shown

the elevated expression of PSMB8 and the potential therapeutic effects of proteasome inhibitors in two mucinous EOC cell lines.

In conclusion, the results of our epigenomics approach lead us to propose that dysregulation of the proteasome system contributes to the pathogenesis of MuOC, COREAD and STAD. We identified PSMB8 as a specific biomarker for MuOC. The application of proteasome inhibitors may

provide a targeted therapy against advanced or recurrent MuOC; therefore, further clinical trials are warranted.

Acknowledgements

None of the authors have any conflicts of interest to declare. They thank the Research Information Section, Office of Information Technology, Taipei Medical University for providing computation services. They also appreciate structural bioinformatics services provided by the TBI Core Facility (<http://www.tbi.org.tw>) and Taipei Medical University Joint Biobank in Taiwan.

References

- Kurman R, Carcangiu M, Herrington C, Young R. World Health Organization classification of tumours of female reproductive organs, 4th edn. World Health Organization, 2014.
- Wang Y, Shwartz L, Anderson D, et al. Molecular analysis of ovarian mucinous carcinoma reveals different cell of origins. *Oncotarget* 2015;6:22949–58.
- Kurman R, Shih I. The dualistic model of ovarian carcinogenesis: revisited, revised, and expanded. *Am J Pathol* 2016;186:733–47.
- Tafe L, Muller K, Ananda G, et al. Molecular genetic analysis of ovarian Brenner tumors and associated mucinous epithelial neoplasms: high variant concordance and identification of mutually exclusive RAS driver mutations and MYC amplification. *Am J Pathol* 2016;186:671–7.
- Winter W, Maxwell G, Tian C, Gynecologic Oncology Group Study, et al. Prognostic factors for stage III epithelial ovarian cancer: a Gynecologic Oncology Group Study. *J Clin Oncol* 2007; 25:3621–7.
- Simons M, Massuger L, Brul J, Bulten J, Teerenstra S, Nagtegaal I. Relatively poor survival of mucinous ovarian carcinoma in advanced stage A systematic review and meta-analysis. *Int J Gynecol Cancer* 2017;
- Heinzelmann-Schwarz V, Gardiner-Garden M, Henshall S, et al. A distinct molecular profile associated with mucinous epithelial ovarian cancer. *Br J Cancer* 2006;94:904–13.
- Mok S, Bell D, Knapp R, et al. Mutation of K-ras protooncogene in human ovarian epithelial tumors of borderline malignancy. *Cancer Res* 1993;53:1489–92.
- Mayr D, Hirschmann A, Lohrs U, et al. KRAS and BRAF mutations in ovarian tumors: a comprehensive study of invasive carcinomas, borderline tumors and extraovarian implants. *Gynecol Oncol* 2006;103:883–7.
- Hunter S, Gorringer K, Christie M, Group. AOCs, Campbell I, et al. Pre-invasive ovarian mucinous tumors are characterized by CDKN2A and RAS pathway aberrations. *Clin Cancer Res* 2012;18: 5267–77.
- Caduff R, Svoboda-Newman S, Ferguson A, et al. Comparison of mutations of Ki-RAS and p53 immunoreactivity in borderline and malignant epithelial ovarian tumors. *Am J Surg Pathol* 1999; 23:323–8.
- Auner V, Kriegshausler G, Tong D, et al. KRAS mutation analysis in ovarian samples using a high sensitivity biochip assay. *BMC Cancer* 2009; 9:111.
- Anglesio M, Kommos S, Tolcher M, et al. Molecular characterization of mucinous ovarian tumors supports a stratified treatment approach with HER2 targeting in 19% of carcinomas. *J Pathol* 2013;229:111–20.
- Gloss B, Samimi G. Epigenetic biomarkers in epithelial ovarian cancer. *Cancer Lett* 2014;342:257–63.
- Balch C, Matei D, Huang T, et al. Role of epigenomics in ovarian and endometrial cancers. *Epigenomics* 2010;2:419–47.
- Reya T, Clevers H. Wnt signalling in stem cells and cancer. *Nature* 2005;434:843–50.
- Liu S, Dontu G, Mantle ID, et al. Hedgehog signaling and Bmi-1 regulate self-renewal of normal and malignant human mammary stem cells. *Cancer Res* 2006;66:6063–71.
- He XC, Zhang J, Tong WG, et al. BMP signaling inhibits intestinal stem cell self-renewal through suppression of Wnt-beta-catenin signaling. *Nat Genet* 2004;36:1117–21.
- Miele L, Miao H, Nickoloff BJ. NOTCH signaling as a novel cancer therapeutic target. *Curr Cancer Drug Targets* 2006;6:313–23.
- Feldmann G, Dhara S, Fendrich V, et al. Blockade of hedgehog signaling inhibits pancreatic cancer invasion and metastases: a new paradigm for combination therapy in solid cancers. *Cancer Res* 2007;67:2187–96.
- Woodward WA, Chen MS, Behbod F, et al. WNT/beta-catenin mediates radiation resistance of mouse mammary progenitor cells. *PNAS* 2007; 104:618–23.
- Ahluwalia A, Hurteau JA, Bigsby RM, et al. DNA methylation in ovarian cancer. II. Expression of DNA methyltransferases in ovarian cancer cell lines and normal ovarian epithelial cells. *Gynecol Oncol* 2001;82:299–304.
- Strathdee G, Appleton K, Illand M, et al. Primary ovarian carcinomas display multiple methylator phenotypes involving known tumor suppressor genes. *Am J Pathol* 2001;158:1121–7.
- Houshdaran S, Hawley S, Palmer C, et al. DNA methylation profiles of ovarian epithelial carcinoma tumors and cell lines. *PLoS One* 2010;5: e9359.
- Teodoridis JM, Hall J, Marsh S, et al. CpG island methylation of DNA damage response genes in advanced ovarian cancer. *Cancer Res* 2005;65: 8961–7.
- Tam KF, Liu VW, Liu SS, Tsang PC, Cheung AN, Yip AM, Ngan HY. Methylation profile in benign, borderline and malignant ovarian tumors. *J Cancer Res Clin Oncol* 2006;
- Furlan D, Carnevali I, Marcomini B, et al. The high frequency of de novo promoter methylation in synchronous primary endometrial and ovarian carcinomas. *Clin Cancer Res* 2006;12:3329–36.
- Wei SH, Balch C, Paik HH, et al. Prognostic DNA methylation biomarkers in ovarian cancer. *Clin Cancer Res* 2006;12:2788–94.
- Huang RL, Gu F, Kirma NB, et al. Comprehensive methylome analysis of ovarian tumors reveals hedgehog signaling pathway regulators as prognostic DNA methylation biomarkers. *Epigenetics* 2013;8:624–34.
- Yamaguchi K, Huang Z, Matsumura N, et al. Epigenetic determinants of ovarian clear cell carcinoma biology. *Int J Cancer* 2014;135:585–97.
- Huang da W, Sherman BT, Lempicki RA. Systematic and integrative analysis of large gene lists using DAVID bioinformatics resources. *Nat Protoc* 2009;4:44–57.
- Huang D. W, Sherman BT, Lempicki RA. Bioinformatics enrichment tools: paths toward the comprehensive functional analysis of large gene lists. *Nucleic Acids Res* 2009;37:1–13.
- Stark C, Breitkreutz BJ, Reguly T, et al. BioGRID: a general repository for interaction datasets. *Nucleic Acids Res* 2006;34:D535–9.
- Hendrix ND, Wu R, Kuick R, et al. Fibroblast growth factor 9 has oncogenic activity and is a downstream target of Wnt signaling in ovarian endometrioid adenocarcinomas. *Cancer Res* 2006; 66:1354–62.
- Liew P, Fang C, Lee Y, et al. DEF6 expression in ovarian carcinoma correlates with poor patient survival. *Diagn Pathol* 2016;11:68–77.
- Tan TZ, Miow QH, Huang RY, et al. Functional genomics identifies five distinct molecular subtypes with clinical relevance and pathways for growth control in epithelial ovarian cancer. *EMBO Mol Med* 2013;5:1051–66.
- Yo YT, Lin YW, Wang YC, et al. Growth inhibition of ovarian tumor-initiating cells by niclosamide. *Mol Cancer Therap* 2012;11:1703–12.
- Kelemen L, Kobel M. Mucinous carcinomas of the ovary and colorectum: different organ, same dilemma. *Lancet Oncol* 2011;12:1071–80.
- Alonso S, González B, Ruiz-Larroja T, et al. Epigenetic inactivation of the extracellular matrix metalloproteinase ADAMTS19 gene and the metastatic spread in colorectal cancer. *Clin Epigenet* 2015;7:124.
- Ryland G, Hunter S, Doyle M, et al. Mutational landscape of mucinous ovarian carcinoma and its neoplastic precursors. *Genome Med* 2015;7: 87.
- Mackenzie R, Kommos S, Winterhoff B, et al. Targeted deep sequencing of mucinous ovarian tumors reveals multiple overlapping RAS-pathway activating mutations in borderline and cancerous neoplasms. *BMC Cancer* 2015;15:415.
- Cildir G, Low KC, Tergaonkar V. Noncanonical NF-kappaB signaling in health and disease. *Trends Mol Med* 2016;22:414–29.
- Wang C, Cicek MS, Charbonneau B, et al. Tumor hypomethylation at 6p21.3 associates with longer

- time to recurrence of high-grade serous epithelial ovarian cancer. *Cancer Res* 2014;74:3084–91.
44. Su H, Lai H, Lin Y, et al. Epigenetic silencing of SFRP5 is related to malignant phenotype and chemoresistance of ovarian cancer through Wnt signaling pathway. *Int J Cancer* 2010;127:555–67.
45. Kitamura A, Maekawa Y, Uehara H, et al. A mutation in the immunoproteasome subunit PSMB8 causes autoinflammation and lipodystrophy in humans. *J Clin Invest* 2011;121:4150–60.
46. Kwon C, Park H, Choi Y, et al. PSMB8 and PBK as potential gastric cancer subtype-specific biomarkers associated with prognosis. *Oncotarget* 2016;7:21454–68.
47. Bazzaro M, Lee M, Zoso A, et al. Ubiquitin-proteasome system stress sensitizes ovarian cancer to proteasome inhibitor-induced apoptosis. *Cancer Res* 2006;66:3754–63.
48. Bazzaro M, Lin Z, Santillan A, et al. Ubiquitin proteasome system stress underlies synergistic killing of ovarian cancer cells by bortezomib and a novel HDAC6 inhibitor. *Clin Cancer Res* 2008;14:7340–7.
49. Aghajanian C, Dizon D, Sabbatini P, et al. Phase I trial of bortezomib and carboplatin in recurrent ovarian or primary peritoneal cancer. *J Clin Oncol* 2005;23:5943–9.
50. Walerych D, Lisek K, Sommaggio R, et al. Proteasome machinery is instrumental in a common gain-of-function program of the p53 missense mutants in cancer. *Nat Cell Biol* 2016;18:897–909.